but are a factor of $2\frac{1}{2}$ larger than the data of Manning *et al.*[4] and Engler *et al.*[5] (not shown), both obtained by a single-arm technique. This discrepancy is large and unexplained. However, Engler *et al.* have stated[5] that systematic errors inherent in the overall normalization of the single-arm technique could be as large as a factor of 2.

The dependence on beam momentum p of $d\sigma/dt$ at fixed t is shown in Fig. 2(b) for our data and those of Friedes *et al.*[3] and Mischke *et al.*[1,2] The error bars in Fig. 2(b) include the estimated relative systematic uncertainty discussed above for our data, and a conservative estimate[7] of the normalization uncertainty in the data of Ref. 2. The solid lines in Fig. 2(b) are the result of fits to our data at four values of t by the form $d\sigma/dt = A(t)p^{-n(t)}$; the dashed lines extrapolate the fits to lower momenta, where they are seen to describe quite well the average p dependence of the Mischke data. The values of n resulting from the fits are shown for all t in the inset to Fig. 2(b). Our data are consistent with a constant value of $n \approx 2.1$ for all $|t|$ between 0.002 and 0.50 $(\mathrm{GeV}/c)^2$. Within errors, there is no indication that the shape of the angular distribution is changing.

We are indebted to Mr. J. Fitch, the engineer responsible for the design and construction of much of the equipment, and to Mr. S. D. Kaynes, II, and Mr. Jay G. Horowitz for aid in software development. We wish to thank Dr. L. G. Ratner who was responsible for the development of the neutron beam. We are grateful to Professor T. A. Romanowski for his encouragement and support, and to Professor G. A. Smith for his contributions during the early stages of the experiment. We wish also to thank the members of the Zero Gradient Synchrotron staff, who at every juncture went out of their way to make our experiment run as smoothly as possible.

*Work supported in part by the U. S. Atomic Energy Commission, by a Science Development Grant from the National Science Foundation, and by the National Research Council of Canada.

[1]R. E. Mischke, P. F. Shepard, and T. J. Devlin, Phys. Rev. Lett. 23, 542 (1969).

[2]P. F. Shepard, T. J. Devlin, R. E. Mischke, and J. Solomon, Princeton-Pennsylvania Accelerator Report No. PPAR-10, 1969 (unpublished).

[3]J. L. Friedes, H. Palevsky, R. L. Stearns, and R. J. Sutter, Phys. Rev. Lett. 15, 38 (1965).

[4]G. Manning, A. G. Parham, J. D. Jafar, H. B. van der Raay, D. H. Reading, D. G. Ryan, B. D. Jones, J. Malos, and N. H. Lipman, Nuovo Cimento 41A, 167 (1966).

[5]J. Engler, K. Horn, F. Mönning, P. Schludecker, W. Schmidt-Parzefall, H. Schopper, P. Sievers, H. Ullrich, R. Hartung, K. Runge, and Yu. Galaktinov, in Proceedings of the Fifteenth International Conference on High Energy Physics, Kiev, U. S. S. R., 1970 (Atomizdat., Moscow, to be published).

[6]R. M. Edelstein, J. Russ, R. C. Thatcher, Mark Elfield, E. L. Miller, N. W. Reay, N. R. Stanton, M. A. Abolins, M. T. Lin, and K. W. Edwards, to be published.

[7]This estimate is based on the error bars in Fig. 23 of Ref. 2; see also the discussion on p.90 of Ref. 2.

Coincidence Measurements of Single π^+ Electroproduction*

C. N. Brown, C. R. Canizares, W. E. Cooper, A. M. Eisner, G. J. Feldman, C. A. Lichtenstein, L. Litt,† W. Lockeretz, V. B. Montana, and F. M. Pipkin

Cyclotron Laboratory, Harvard University, Cambridge, Massachusetts 02138

(Received 17 February 1971)

We have studied the reaction $e^- + p \rightarrow e^- + \pi^+ + n$ by detecting the final electron and pion in coincidence. Data are presented in the region of virtual photon mass squared from -0.18 to -1.2 GeV^2, and virtual photoproduction center-of-mass energy and angle from 1.85 to 2.50 GeV and 0 to 20°, respectively.

We have performed a series of experiments at the Cambridge Electron Accelerator (CEA) to study electroproduction by detecting a charged hadron in coincidence with the scattered electron. This Letter presents our results for the reaction $e^- + p \rightarrow e^- + \pi^+ + n$.

To lowest order in the electromagnetic interaction this process can be treated as photoproduction by a virtual photon whose mass, energy, direction, and polarization density matrix are tagged by the detected electron. The cross section can then be written[1]

$$\frac{d^3\sigma}{dE'd\Omega_e d\Omega_\pi} = \Gamma \frac{d\sigma}{d\Omega_\pi}, \tag{1}$$

where Γ represents the flux of virtual photons,

and (if no external polarizations are measured) the virtual photoproduction cross section is given by

$$\frac{d\sigma}{d\Omega_\pi} = A + \epsilon B \cos 2\varphi + \epsilon C + [\epsilon(1+\epsilon)/2]^{1/2} D \cos\varphi. \quad (2)$$

A, B, C, and D are functions of three variables: k^2, the mass squared of the virtual photon; W, the total energy of the pion and neutron in their center-of-mass system; and θ, the polar angle between the virtual photon and the pion in the pion-neutron center-of-mass frame. An alternate variable is t, the invariant momentum difference squared between the virtual photon and the pion. φ is the azimuthal angle between the electron scattering plane and the pion photoproduction plane. The phase of φ is such that if the pion were emitted along the direction of the incident electron, φ would be zero.

The polarization factor ϵ which characterizes the photon density matrix can be expressed in terms of the incident and scattered electron energies (E and E') and the laboratory electron scattering angle (θ_e) by

$$\epsilon = \{1 + 2[1-(E-E')^2/k^2]\tan^2(\theta_e/2)\}^{-1}. \quad (3)$$

Γ is given in terms of these variables by[2]

$$\Gamma = \frac{\alpha}{2\pi^2}\frac{E'}{E}\frac{W^2-M^2}{2M}\frac{1}{-k^2}\frac{1}{1-\epsilon}. \quad (4)$$

In Eq. (2), A is the cross section for unpolarized transverse photons, B is the contribution due to transverse polarization, C is the cross section for scalar photons, and D is the scalar-transverse interference term. B and D must vanish at $\theta = 0$, and C and D must vanish at $k^2 = 0$.

Data were collected in three scans. In each scan we varied the central setting of the apparatus for one of the three variables, k^2, W, and θ, and kept the remaining two fixed. The central settings of k^2 ranged from -0.18 to -1.2 GeV^2 for $W = 2.15$ GeV and $\theta = 0°$; the central settings of W ranged from 1.85 to 2.50 GeV for $k^2 = -0.3$ GeV^2 and $\theta = 0°$; and the central settings for θ ranged from 0° to 15° for $k^2 = -0.40$ GeV^2 and $W = 2.15$ GeV. Previous experiments[3,4] have studied the region of the first resonance, $W \approx 1.24$ GeV, for $-k^2 < 0.4$ GeV^2.

Our angular scan was confined to values of φ corresponding to pion production near the electron scattering plane; i.e., to φ near 0° and φ near 180°. Typically, ϵ was 0.8 to 0.9. Because data were taken at fixed ϵ, we could not separate A and C of Eq. (2). B could be separated only at small θ.[5]

In our experimental arrangement, the CEA external electron beam was incident upon a 15.9-cm liquid-hydrogen target and was measured downstream with a Faraday cup. The electron and pion were detected in separate arms of a two-arm magnetic spectrometer. The two arms were mirror images of each other; a schematic diagram of one is shown in Fig. 1. Each arm consisted of a horizontally focusing half-quadrupole, a vertical bending magnet, a vertically focusing half-quadrupole, and detection equipment. The latter included five wire spark-chamber modules, three scintillation trigger counters, a scintillation-counter hodoscope, a threshold Cherenkov counter filled with Freon 12, and a shower counter (used for diagnostic purposes only). The spark-chamber modules each contained four planes with magnetostrictive readout. The Cherenkov counter on the electron-detecting arm was set to count electrons but not pions, and the one on the pion-detecting arm was set to count pions but not K's or protons. The spark chambers were fired on two-arm coincidences. The data were logged by an SDS 92-IBM

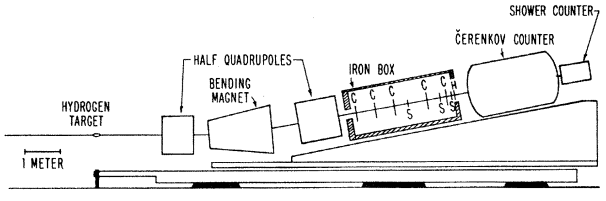

FIG. 1. Schematic diagram showing side view of one spectrometer. C denotes a wire spark-chamber module, S denotes a trigger counter, and H denotes a hodoscope.

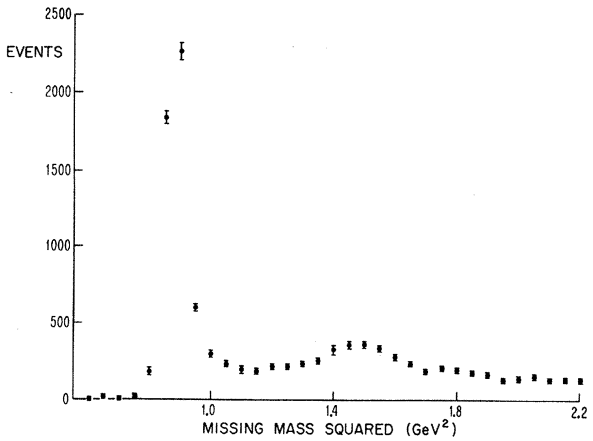

FIG. 2. Typical missing-mass-squared spectrum when electrons and pions are detected in coincidence.

Table I. Angular distributions of virtual-photoproduction cross sections and transverse-scalar interference term D. Units are μb/sr and uncertainties are statistical only.

W(GeV)	2.15			2.31			2.02		
k^2(GeV^2)	-.396			-.354			-.426		
ϵ	.870			.818			.901		
	$d\sigma/d\Omega_\pi$	$d\sigma/d\Omega_\pi$		$d\sigma/d\Omega_\pi$	$d\sigma/d\Omega_\pi$		$d\sigma/d\Omega_\pi$	$d\sigma/d\Omega_\pi$	
θ	$\varphi=0^\circ$	$\varphi=180^\circ$	D	$\varphi=0^\circ$	$\varphi=180^\circ$	D	$\varphi=0^\circ$	$\varphi=180^\circ$	D
0.8°	9.02±.68[a]			8.29±.78[a]			11.11±.91[a]		
1.8°	10.43±1.09	8.54±1.00	1.04±.85	9.77±1.04	6.61±.99	1.84±.86	13.22±1.47	10.12±1.17	1.68±1.05
3.0°	10.14± .84	7.41± .73	1.51±.64	8.76± .72	4.55±.67	2.44±.58	11.81±1.02	9.24± .86	1.39± .74
4.2°	10.98± .79	7.22± .62	2.08±.57	9.14± .61	5.62±.74	2.04±.57	11.63± .86	8.99± .72	1.43± .62
5.4°	9.44± .68	7.34± .59	1.15±.51	7.50± .47	4.14±.50	1.95±.41	10.81± .74	8.22± .60	1.40± .53
6.6°	8.69± .61	6.21± .49	1.38±.44	7.47± .40	4.70±.45	1.61±.36	9.91± .66	7.61± .52	1.24± .46
7.8°	7.58± .56	5.71± .45	1.03±.40	7.02± .38	4.55±.43	1.44±.34	8.65± .61	7.08± .44	.85± .42
9.0°	7.22± .55	5.35± .41	1.03±.39	4.83± .47	4.36±.44	.27±.38	9.19± .64	6.78± .41	1.30± .42
10.2°	7.35± .53	5.38± .39	1.09±.37		4.12±.44		8.10± .61		
11.4°	6.51± .50	5.08± .37	.79±.35		4.87±.53		7.54± .64		
12.6°	4.71± .41	4.24± .31	.26±.29		3.09±.37		6.11± .60		
13.8°	4.18± .36	4.18± .30	.00±.26		2.42±.35		4.95± .55		
15.0°	3.40± .32	3.68± .28	-.16±.24		3.54±.40		3.85± .50		
16.2°					2.61±.33		3.67± .49		
17.4°							3.35± .43		
18.6°							3.01± .43		
19.8°							2.25± .32		

[a]Values at 0.8° are averages over all φ.

360/65 time-sharing system.

The momentum acceptance of each arm was approximately ±30%. The rms momentum resolution was 10 MeV/c and was dominated by multiple scattering. The angular acceptances were 1° in the horizontal direction and 2° in the vertical direction.

A time-of-flight system with an rms resolution of 0.55 nsec was used to separate a large background of accidental arm-to-arm coincidences. This background was analyzed in order to correct the data for those accidentals which could not be separated.

We separated the π^+n channel from other final states by computing the mass of the undetected particle(s). A typical missing-mass-squared spectrum after subtraction of accidentals is shown in Fig. 2; the rms resolution is 0.03 GeV^2. Only events within 0.12 GeV^2 of the neutron peak were analyzed to obtain the results presented in this Letter.

Corrections were made for the following: chamber recovery deadtime (4 to 48%), radiative processes[6] (≈29%), target bremsstrahlung[7] (≈15%), pion decay (4 to 12%), pion absorption (3 to 6%), pion pair misidentification (0 to 10%), scattering from magnet poles (2 to 5%), target-empty rates (≈1%), counter deadtimes (≈1%), chamber and counter inefficiencies (≈1%), and other small effects. Uncertainties in these corrections result in a possible systematic error of ≈5%.

Data from the θ, W, and k^2 scans are presented in Tables I, II, and III, respectively. The data are tabulated in terms of virtual photoproduction cross sections, as defined by Eq. (1). All are quoted with statistical uncertainties only. Except for the angular scan in Table I, there is a high degree of correlation between values of W, k^2, ϵ, and θ for each spectrometer setting. This is a consequence of the strong dependence of the virtual photon's momentum, direction, and polarization upon the momentum of the detected electron.

One may draw several rather general conclusions from these data. The W dependences at fixed θ (Table II) are consistent with an absence of strong resonance effects. A significant feature of the k^2 scan is the initial rise of the 0° cross sections with increasing $-k^2$ (Table III).

Table II. W dependence of small-angle virtual-photoproduction cross sections. Uncertainties are statistical only.

$0^\circ \le \theta \le 2.4^\circ$ $k^2 = -.29$ GeV^2

W(GeV)	$\frac{d\sigma}{d\Omega_\pi}(\frac{\mu b}{sr})$	ϵ
1.84	12.81±.83	.94
2.05	9.68±.61	.92
2.14	8.69±.35	.89
2.50	4.99±.17	.73

$2.4^\circ \le \theta \le 4.8^\circ$, $\varphi \approx 0^\circ$, $k^2 = -.30$ GeV^2

W(GeV)	$\frac{d\sigma}{d\Omega_\pi}(\frac{\mu b}{sr})$	ϵ	$\cos\varphi$	$\cos 2\varphi$
1.79	14.47±.94	.95	.83	.44
1.98	11.80±.70	.93	.84	.47
2.07	11.31±.44	.91	.86	.55
2.41	7.91±.26	.78	.87	.60

$2.4^\circ \le \theta \le 4.8^\circ$, $\varphi \approx 180^\circ$, $k^2 = -.28$ GeV^2

W(GeV)	$\frac{d\sigma}{d\Omega_\pi}(\frac{\mu b}{sr})$	ϵ	$\cos\varphi$	$\cos 2\varphi$
1.90	10.65±.73	.94	-.83	.42
2.12	6.92±.55	.90	-.83	.41
2.22	5.63±.32	.86	-.84	.45
2.60	2.26±.15	.68	-.88	.58

$4.8^\circ \le \theta \le 9.6^\circ$, $\varphi \approx 0^\circ$, $k^2 = -.31$ GeV^2

W(GeV)	$\frac{d\sigma}{d\Omega_\pi}(\frac{\mu b}{sr})$	ϵ	$\cos\varphi$	$\cos 2\varphi$
1.74	14.52±.68	.96	.91	.67
1.92	10.35±.47	.94	.92	.73
2.01	10.71±.32	.92	.94	.79
2.31	6.76±.30	.82	.97	.87

$4.8^\circ \le \theta \le 9.6^\circ$, $\varphi \approx 180^\circ$, $k^2 = -.26$ GeV^2

W(GeV)	$\frac{d\sigma}{d\Omega_\pi}(\frac{\mu b}{sr})$	ϵ	$\cos\varphi$	$\cos 2\varphi$
1.96	9.20±.44	.93	-.90	.63
2.20	4.39±.33	.88	-.93	.75
2.31	4.41±.24	.85	-.94	.78
2.71	1.90±.20	.61	-.98	.91

Table III. k^2 dependence of small-angle virtual-photoproduction cross sections. Uncertainties are statistical only.

$0^\circ \le \theta \le 2.4^\circ$ $W = 2.15$

k^2(GeV^2)	ϵ	$\frac{d\sigma}{d\Omega_\pi}$(μb/sr)
- .176	.853	7.18±.34
- .294	.880	8.28±.45
- .396	.870	9.09±.35
- .795	.830	7.02±.37
-1.188	.788	3.55±.28

$2.4^\circ \le \theta \le 4.8^\circ$ $\varphi \approx 0^\circ$ $\cos\varphi \approx .87$ $\cos 2\varphi \approx .56$

k^2(GeV^2)	W(GeV)	ϵ	$\frac{d\sigma}{d\Omega_\pi}$(μb/sr)
- .189	2.070	.878	10.25±.47
- .308	2.083	.896	11.51±.57
- .411	2.088	.886	11.12±.44
- .825	2.096	.844	6.51±.40
-1.232	2.110	.802	4.06±.35

$2.4^\circ \le \theta \le 4.8^\circ$ $\varphi \approx 180^\circ$ $\cos\varphi \approx -.84$ $\cos 2\varphi \approx .47$

k^2(GeV^2)	W(GeV)	ϵ	$\frac{d\sigma}{d\Omega_\pi}$(μb/sr)
- .166	2.226	.822	3.48±.32
- .281	2.224	.856	5.43±.42
- .379	2.218	.850	6.85±.34
- .768	2.203	.814	5.74±.38
-1.144	2.208	.770	3.70±.33

This cross section has the form $A + \epsilon C$, where the scalar contribution C must vanish as $k^2 \to 0$. If, as is plausible, the purely transverse part A monotonically decreases with $-k^2$, then our results imply a significant scalar component. (The data are not plotted because of the variation of ϵ from point to point.)

Just how large the scalar component actually is must be determined by utilizing some specific model. For those models which include a contribution from a t-channel pion pole, the size of that component is related to the pion form factor. One may thus hope to extract the latter in a mod-

el-dependent way. For this procedure to be meaningful, such a model must be able to reproduce our observed angular distributions (Table I). In particular, the most sensitive test our data can provide is the requirement that a model predict the correct interference term, D, because that term involves both scalar and transverse amplitudes.

A detailed comparison with a particular model is given in the following Letter.[8]

We gratefully acknowledge the support and cooperation of the director and staff of the CEA. We also wish to thank the staff of the Harvard Cyclotron Laboratory for their invaluable assistance.

---

*Research supported by the U. S. Atomic Energy Commission under Contract No. AT(30-1)-2752.

†Junior Fellow, Society of Fellows.

[1]J. K. Randolph, unpublished; C. W. Akerlof, W. W. Ash, K. Berkelman, and M. Tigner, Phys. Rev. Lett. 14, 1036 (1965). See also H. F. Jones, Nuovo Cimento 40A, 1018 (1965); N. Dombey, Rev. Mod. Phys. 41, 236 (1969).

[2]We adopt a normalization convention introduced by L. N. Hand, Phys. Rev. 129, 1834 (1963).

[3]C. W. Akerlof, W. W. Ash, K. Berkelman, C. A. Lichtenstein, A. Ramanauskas, and R. H. Siemann, Phys. Rev. 163, 1482 (1967).

[4]C. Mistretta, J. A. Appel, R. J. Budnitz, L. Carroll, J. Chen, J. R. Dunning, Jr., M. Goitein, K. Hanson, D. C. Imrie, and R. Wilson, Phys. Rev. 184, 1487 (1969).

[5]In terms of the conventional Cartesian notation for transverse, polarized photoproduction cross sections, A and B are equivalent to $(d\sigma_{\parallel}/d\Omega_{\pi}+d\sigma_{\perp}/d\Omega_{\pi})/2$ and $(d\sigma_{\parallel}/d\Omega_{\pi}-d\sigma_{\perp}/d\Omega_{\pi})/2$, respectively. Since ϵ and $\cos 2\varphi$ are both close to 1, our experiment is much more sensitive to the parallel polarization than to the perpendicular one.

[6]A. Bartl and P. Urban, Acta Phys. Austr. 24, 139 (1966); A. Bartl and F. Widder, private communication. There are several misprints in the published work.

[7]L. W. Mo and Y. S. Tsai, Rev. Mod. Phys. 41, 205 (1969). Corrections to this paper have been brought to our attention by E. Bloom, M. Breidenbach, J. Friedman, P. Kirk, and G. Miller, private communications.

[8]C. N. Brown, C. R. Canizares, W. E. Cooper, A. M. Eisner, G. J. Feldman, C. A. Lichtenstein, L. Litt, W. Lockeretz, V. B. Montana, and F. M. Pipkin, following Letter [Phys. Rev. Lett. 26, 991 (1971)].

Interpretations of Single π^+ Electroproduction Data and a Determination of the Pion Form Factor*

C. N. Brown, C. R. Canizares, W. E. Cooper, A. M. Eisner, G. J. Feldman, C. A. Lichtenstein, L. Litt,† W. Lockeretz, V. B. Montana, and F. M. Pipkin

Cyclotron Laboratory, Harvard University, Cambridge, Massachusetts 02138

(Received 17 February 1971)

New data on forward π^+ electroproduction are in reasonable agreement with the predictions of a dispersion-theory calculation by Berends. This model is used to extract the pion electromagnetic form factor. The result is consistent with $F_\pi = F_1^V$, but a simple ρ-pole form factor cannot be ruled out.

High-energy π^+ photoproduction has shown remarkably simple behavior in the region of small momentum transfer.[1] The data are qualitatively described by Born terms, and are well fitted by including corrections based on low-energy behavior.[2,3] This approach has been extended from real to virtual photoproduction by Berends.[4]

In the preceeding Letter,[5] we obtained cross sections for the virtual photoproduction of single π^+ mesons by analyzing data on the electroproduction reaction $e^- + p \to e^- + \pi^+ + n$. In that Letter Berends's predictions are compared with our measurements. Conventions and notation will be those of Ref. 5.

The amplitudes constructed by Berends contain the pion- and nucleon-pole terms (the "generalized Born approximation") and a fixed-t dispersion integral. The amplitudes are assumed to be isovector and purely real for our energy region, and only the M_{1+}[3] multipole of the $\Delta(1236)$ is included in the integral. With these assumptions, the pion form factor, $F_\pi(k^2)$, is the only free parameter in the theory. For $-t < 3m_\pi^2$ and $W > 2$ GeV the theory agrees reasonably well with real-photoproduction data.[6]

Figure 1(a) shows the angular distribution of our data at $W = 2.15$ GeV, $k^2 = -0.396$ GeV^2, and $\epsilon = 0.87$ for $\varphi = 0°$ and $\varphi = 180°$. The curves represent Berends's theory with $F_\pi = F_1^V$ (=0.566 here).[7] Fits have been made to these data with F_π as a free parameter. If angles up to 7° ($t \approx -m_\pi^2$) are included, F_1^V gives close to a best fit, with a χ^2